ANNALS of Clinical and Translational Neurology
Open Access
ANA American Neurological Association since 1875

RESEARCH ARTICLE

Investigation of white matter PiB uptake as a marker of white matter integrity

Burcu Zeydan[1,2,3], Christopher G. Schwarz[1], Val J. Lowe[1], Robert I. Reid[4], Scott A. Przybelski[5], Timothy G. Lesnick[5], Walter K. Kremers[5], Matthew L. Senjem[1,4], Jeffrey L. Gunter[1,4], Hoon-Ki Min[1], Prashanthi Vemuri[1], David S. Knopman[2], Ronald C. Petersen[2], Clifford R. Jack Jr[1], Orhun H. Kantarci[2,3] & Kejal Kantarci[1]

[1]Department of Radiology, Mayo Clinic, Rochester, Minnesota
[2]Department of Neurology, Mayo Clinic, Rochester, Minnesota
[3]Center for Multiple Sclerosis and Autoimmune Neurology, Mayo Clinic, Rochester, Minnesota
[4]Department of Information Technology, Mayo Clinic, Rochester, Minnesota
[5]Department of Health Sciences Research, Mayo Clinic, Rochester, Minnesota

Correspondence
Kejal Kantarci, Department of Radiology, Mayo Clinic and Foundation, 200 First Street, SW, Rochester, MN 55905. Tel: +1 507 284 9770; Fax: +1 507 284 9778; E-mail: kantarci.kejal@mayo.edu

Funding Information
This study was funded by the National Institutes of Health (NIH) [R01 AG040042, P50 AG016574, U01 AG006786, RF1 AG57547, C06 RR018898, R01 AG034676, R01 AG011378, R01 AG041851, R01 NS097495], the Elsie and Marvin Dekelboum Family Foundation, the Robert H. and Clarice Smith and Abigail Van Buren Alzheimer's Disease Research Program, the GHR Foundation, Mayo Foundation for Medical Education and Research, the Schuler Foundation and the Alexander Family Alzheimer's Disease Research Professorship of the Mayo Clinic. The funding sources had no role in study design, collection, analysis, interpretation, or decision to submit this paper.

Received: 4 October 2018; Revised: 14 January 2019; Accepted: 3 February 2019

Annals of Clinical and Translational Neurology **2019; 6(4): 678–688**

doi: 10.1002/acn3.741

Abstract

Objective: To investigate the associations of Pittsburgh compound-B (PiB) uptake in white matter hyperintensities (WMH) and normal appearing white matter (NAWM) with white matter (WM) integrity measured with DTI and cognitive function in cognitively unimpaired older adults. **Methods**: Cognitively unimpaired older adults from the population-based Mayo Clinic Study of Aging (n = 537, age 65–95) who underwent both PiB PET and DTI were included. The associations of WM PiB standard uptake value ratio (SUVr) with fractional anisotropy (FA) and mean diffusivity (MD) in the WMH and NAWM were tested after adjusting for age. The associations of PiB SUVr with cognitive function z-scores were tested after adjusting for age and global cortical PiB SUVr. **Results**: The WMH PiB SUVr was lower than NAWM PiB SUVr ($P < 0.001$). In the WMH, lower PiB SUVr correlated with lower FA ($r = 0.21$, $P < 0.001$), and higher MD ($r = -0.31$, $P < 0.001$). In the NAWM, lower PiB SUVr only correlated with higher MD ($r = -0.10$, $P = 0.02$). Both in the WMH and NAWM, lower PiB SUVr was associated with lower memory, language, and global cognitive function z-scores after adjusting for age and global cortical PiB SUVr. **Interpretation**: Reduced PiB uptake in the WMH is associated with a loss of WM integrity and cognitive function after accounting for the global cortical PiB uptake, suggesting that WM PiB uptake may be an early biomarker of WM integrity that precedes cognitive impairment in older adults. When using WM as a reference region in cross-sectional analysis of PiB SUVr, individual variability in WMH volume as well as age should be considered.

Introduction

White matter (WM) Pittsburgh compound-B (PiB) uptake is increasingly being used as a reference region to calculate the PiB standard uptake value ratios (SUVr) in longitudinal PET imaging studies,[1–5] as an alternative to PiB uptake in the cerebellum. However, the basis of PiB uptake in the WM is not fully understood. WM PiB uptake increases with age, with a parallel increase in global cortical PiB uptake.[6] On the other hand, β-amyloid PET tracer uptake is lower in demyelinating lesions[7–12] as well as in nonspecific WM hyperintensities (WMH) in

older adults.[13,14] Studies of PiB uptake in demyelinating and remyelinating WM lesions in animal models[9] and patients with multiple sclerosis (MS)[11] have suggested that WM PiB uptake may be used as an imaging biomarker for myelin integrity if age correction is employed. We recently showed that PiB uptake is lower in WMH than in normal appearing WM (NAWM) in patients with MS.[12] Furthermore, PiB uptake in the WMH, and also in the NAWM correlated with cognitive function in patients with MS.[12] These earlier studies in patients with MS suggest that PiB uptake may be utilized as a biomarker of WM integrity, particularly for detection of early neurodegenerative alterations in the WM that precedes cognitive impairment in older adults.

Fractional anisotropy (FA) and mean diffusivity (MD) on diffusion tensor MRI (DTI) are well-known imaging biomarkers for the density of axons and myelin in the WM.[15,16] Therefore, WM FA and MD measurements may help understand the basis of PiB uptake in the WM. In the current study, we investigated the PiB uptake in the WMH and NAWM in cognitively unimpaired older adults and the relationships of WMH and NAWM PiB uptake with age, FA and MD on DTI, and cognitive function. We hypothesized that lower PiB uptake values in the WMH and NAWM would be associated with lower FA and higher MD values on DTI and lower cognitive performance.

Methods

Study population

Participants from the Mayo Clinic Study of Aging (MCSA), which is a prospective population-based study of cognitive aging,[17] were included. Clinical evaluation and neuropsychological testing were performed to identify cognitively unimpaired older adults (age 65–95) who underwent both PiB PET and MRI that included a DTI scan (n = 537). Briefly, all raw cognitive test scores were standardized in the MCSA 50+ population using the baseline cognitively unimpaired enrollment visits between the years 2004–2012 and weighted to the Olmsted County population. The neuropsychological testing assessed four cognitive domains of memory, language, attention-executive function, and visual-spatial skills as previously described.[17] The average of individual domain z-scores was used to calculate a global cognitive function z-score.[17] Cognitively unimpaired participants were classified based upon a consensus diagnosis by physicians, neuropsychologists, and study coordinators who evaluated the participants.

The study protocol was approved by the Institutional Review Boards and all participants signed informed consent.

MRI methods

MRIs were performed on 3.0 Tesla scanners (GE, Milwaukee, WI, USA). A T2-weighted fluid-attenuated inversion recovery (FLAIR) and a T1-weighted 3D high resolution magnetization-prepared rapid acquisition gradient-echo (MPRAGE) sequence (TR/TE/T1, 2300/3/900 msec, spatial resolution = $1 \times 1 \times 1.2$ mm^3, slice thickness of 1.2 mm, flip angle 8°, 26-cm field of view)[18] were included in the standardized protocol for anatomic segmentation and labeling of WMH and NAWM on the PiB PET and DTI images. WM was segmented into WMH and NAWM using a semiautomated segmentation algorithm on FLAIR-MRI as previously described.[19] FLAIR images were registered to the corresponding MPRAGE using SPM12, and the corresponding WMH segmentations were transformed using these same parameters. The minimal size for the WMH that was detected in FLAIR-MRI was approximately 5 mm^3.

MPRAGE images were segmented using SPM12[20] with the Mayo Clinic Adult Lifespan Template (https://www.nitrc.org/projects/mcalt/).[21] These segmentations were used to generate a WM mask by thresholding the SPM12 WM segmentation to include those voxels with $P \geq 0.5$. Any voxels segmented as WMH in the coregistered, resampled FLAIR images were also included as WM to account for T1-hypointense lesions being erroneously called gray matter. We then eroded this WM segmentation mask by three voxels, to exclude those voxels most severely affected by partial volume averaging of cerebrospinal fluid (CSF) and gray matter (i.e., U-fibers and periventricular voxels). Remaining WM voxels were then used for all analyses. These WM voxels were split into two subclass masks: those segmented as WMH, and all others, which we called NAWM.

A single-shot echo-planar DTI pulse sequence was performed with a SENSE factor of two in the axial plane. The DTI sequence's parameters were TE = 68 msec; TR = 10,200 msec; an in-plane matrix of 128/128; field of view 35 cm, and 2.7 mm as the slice thickness for 2.7 mm isotropic resolution. The DTI volumes consisted of 41 diffusion-encoding gradient directions and a set of five of nondiffusion T2-weighted volumes (b0s). Diffusion MRI brain voxels were segmented using an automated method.[22] After correcting for subject motion and residual eddy current distortion, diffusion tensors were fit on extracted brain voxels using weighted least squares optimization and FA and MD images were calculated from eigenvalues of the tensors using Dipy.[23] DTI FA and MD images were registered to the T1-weighted image using SPM12 by using the average b0 image to compute an affine transformation for DTI and applying this to the FA and MD images.

PiB PET methods

PET/CT scanner (Discovery, GE Healthcare, Waukesha, WI) operating in three-dimensional mode was used for PiB PET imaging. The participants were injected with PiB (target injection dose = 15 mCi [555 MBq]) and after waiting for an uptake period of 40 min, a PiB scan was acquired as four 5-min of dynamic frames that were checked for motion and averaged to create a static PiB PET image. The full width at half maximum of the PET scanners' point spread function was approximately 4–5 mm in air, and approximately 8 mm in water phantoms.[24] Further, a standard iterative reconstruction (256 matrix, 300 mm field of view, 1.17 × 1.17 × 3.27 mm voxel size) with corrections for attenuation, scatter, random coincidences, and radioactive decay were applied as well as a 5-mm Gaussian postfilter as previously described.[1] PiB PET image analysis was performed using an automated image processing pipeline, which was previously described.[18] The cerebellar crus gray matter was used as a reference region to create normalized PiB PET standardized uptake value ratio (SUVr) images. To calculate the global cortical PiB SUVr, a mask of the bilateral temporal, parietal, prefrontal, orbitofrontal and anterior cingulate gray matter regions was used.

Finally, the mean value for each of DTI FA and PiB PET SUVr over all voxels in each of the WMH and NAWM segmentation masks was computed.

Statistical analysis

PiB SUVr, FA and MD were compared between WMH and NAWM using paired *t*-tests to account for the within-subject matching. Pearson correlations were used to test for associations of PiB SUVr, FA and MD with age in WMH and NAWM. Regression models and partial Pearson correlations were used to test for associations of PiB SUVr with FA and MD in the WMH and NAWM, after adjusting for age, since age significantly influences WM PiB SUVr,[6] FA,[25,26] and MD.[26] We used mixed effects models to compare (1) associations of each imaging biomarker (PiB SUVr, FA and MD) with age between WMH and NAWM; (2) associations of PiB SUVr with FA and MD between WMH and NAWM, adjusted for age, with all of the PiB SUVr, FA and MD in the data, and two values per subject according to WMH or NAWM. The mixed effects models accounted for within-subject correlations. We used a group variable for WMH/NAWM, where 0 = WMH and 1 = NAWM, and tested for an interaction by group. A significant interaction would indicate a difference in slopes for WMH and NAWM. Regression models and partial Pearson correlations were also used to test for associations of PiB SUVr, in the WMH and NAWM with memory, language, attention-executive function, visual-spatial function and global cognitive function *z*-scores. Because age significantly influences WM PiB SUVr,[6] and both age and global cortical PiB SUVr influence cognitive function,[27,28] the associations of PiB SUVr with cognitive function domain *z*-scores were tested in these models after adjusting for both age and global cortical PiB SUVr. Assumptions underlying the regression models were assessed using standard analysis of the residuals, and assumptions underlying the mixed models were assessed using methods from Fox and Weisberg (2014).[29]

Results

Demographics and characteristics of participants

The mean age of the cohort at time of imaging was 75.9 ± 7.3 years. Of the participants, 43% were women and 29% were *APOE ε4* carriers. The short test of mental status[30] [mean ± standard deviation (SD) = 35.4 ± 2.0], clinical dementia rating scale sum of boxes (mean ± SD = 0.05 ± 0.23) and global cognitive function test *z*-score (mean ± SD = 0.15 ± 0.86) were within normal limits (Table 1). On the MRI, the mean WMH volume was 18.06 ± 17.39 cc, and as expected, the WMH volume increased with age ($r = 0.54$, $P < 0.001$). The mean ± SD global cortical PiB SUVr was 1.49 ± 0.42.

PiB uptake, FA, and MD in the WMH and NAWM

The WMH PiB SUVr (mean ± SD = 1.88 ± 0.20) was lower compared to NAWM PiB SUVr (mean ± SD =

Table 1. Participants' characteristics.

	n = 537
Age, years	75.9 (7.3)
Women (%)	231 (43%)
Education, years	14.7 (2.6)
APOE ε4 carrier status (%)	156 (29%)
Short test of mental status[30]	35.4 (2.0)
CDR sum of boxes	0.05 (0.23)
Memory function *z*-score	0.23 (1.01)
Language function *z*-score	0.02 (0.90)
Attention-executive function *z*-score	−0.09 (0.86)
Visual-spatial function *z*-score	0.23 (0.88)
Global cognitive function *z*-score	0.15 (0.86)
Global cortical PiB SUVr	1.49 (0.42)
White matter hyperintensity volume, cc	18.06 (17.39)

Mean (standard deviation) for the continuous variables and count (%) for the categorical variables.
CDR, clinical dementia rating scale; PiB, Pittsburgh compound-B; SUVr, standard uptake value ratio.

2.08 ± 0.20) using paired *t*-tests ($P < 0.001$) (Fig. 1). Both the WMH and NAWM PiB SUVrs increased with age ($P < 0.001$) (Table 2), but this relationship was steeper in the NAWM compared to WMH using mixed effects models (differences in slopes $P < 0.001$) (Table S1). On DTI, the WMH FA (mean ± SD = 0.37 ± 0.05) was lower compared to NAWM FA (mean ± SD = 0.45 ± 0.02), and the WMH MD (mean ± SD = 921 ± 99 × 10^{-6} mm^2/sec) was higher compared to NAWM MD (mean ± SD = 755 ± 35 × 10^{-6} mm^2/sec) using paired *t*-tests ($P < 0.001$) (Fig. 1). Both the WMH FA and NAWM FA decreased with age ($P < 0.001$) (Table 2), and this relationship was steeper in the WMH than in the NAWM using mixed effects models (differences in slopes $P < 0.001$) (Table S1). Both the WMH MD and NAWM MD increased with age ($P < 0.001$) (Table 2), and this relationship was steeper in the WMH than in the NAWM using mixed effects models (differences in slopes $P < 0.001$) (Table S1).

Lower PiB SUVr correlated with lower FA in the WMH ($r = 0.21$, $P < 0.001$), but not in the NAWM ($r = 0.07$, $P = 0.10$) after adjusting for age. Lower PiB SUVr correlated with higher MD both in the WMH ($r = -0.31$, $P < 0.001$), and NAWM ($r = -0.10$, $P = 0.02$) after adjusting for age (Table 2, Fig. 2). However, we did not observe a difference in slopes of the associations of PiB SUVr and MD in the WMH with the NAWM ($P = 0.34$) using mixed effects models (Table S1).

Higher WMH PiB SUVr correlated with higher NAWM PiB SUVr ($r = 0.94$, $P < 0.001$), after adjusting for age. Similarly, higher WMH FA correlated with higher NAWM FA ($r = 0.48$, $P < 0.001$), and higher WMH MD correlated with higher NAWM MD ($r = 0.67$, $P < 0.001$), after adjusting for age. Higher global cortical PiB SUVr correlated with higher PiB SUVr both in the WMH ($r = 0.20$, $P \leq 0.001$) and NAWM ($r = 0.25$, $P \leq 0.001$), after adjusting for age. While WMH volume did not correlate with WMH PiB SUVr ($r = -0.069$, $P = 0.11$), higher WMH volume correlated with lower WMH FA ($r = -0.69$, $P \leq 0.001$) and higher WMH MD ($r = 0.83$, $P \leq 0.001$). In Figure 3, examples of PiB PET, DTI, T2-FLAIR and MPRAGE MRIs of two

Table 2. Associations of Pittsburgh compound-B standard uptake value ratio and diffusion tensor imaging fractional anisotropy and mean diffusivity in the white matter hyperintensities and normal appearing white matter.

Pearson correlations	WMH R (*P*)	NAWM R (*P*)
PiB SUVr and age	0.14 (<0.001)	0.28 (<0.001)
FA and age	−0.35 (<0.001)	−0.17 (<0.001)
MD and age	0.48 (<0.001)	0.46 (<0.001)
FA and PiB SUVr, adjusted for age	0.21 (<0.001)	0.07 (0.10)
MD and PiB SUVr, adjusted for age	−0.31 (<0.001)	−0.10 (0.02)

FA, fractional anisotropy; MD, mean diffusivity; NAWM, normal appearing white matter; PiB, Pittsburgh compound-B; SUVr, standard uptake value ratio; WMH, white matter hyperintensity.

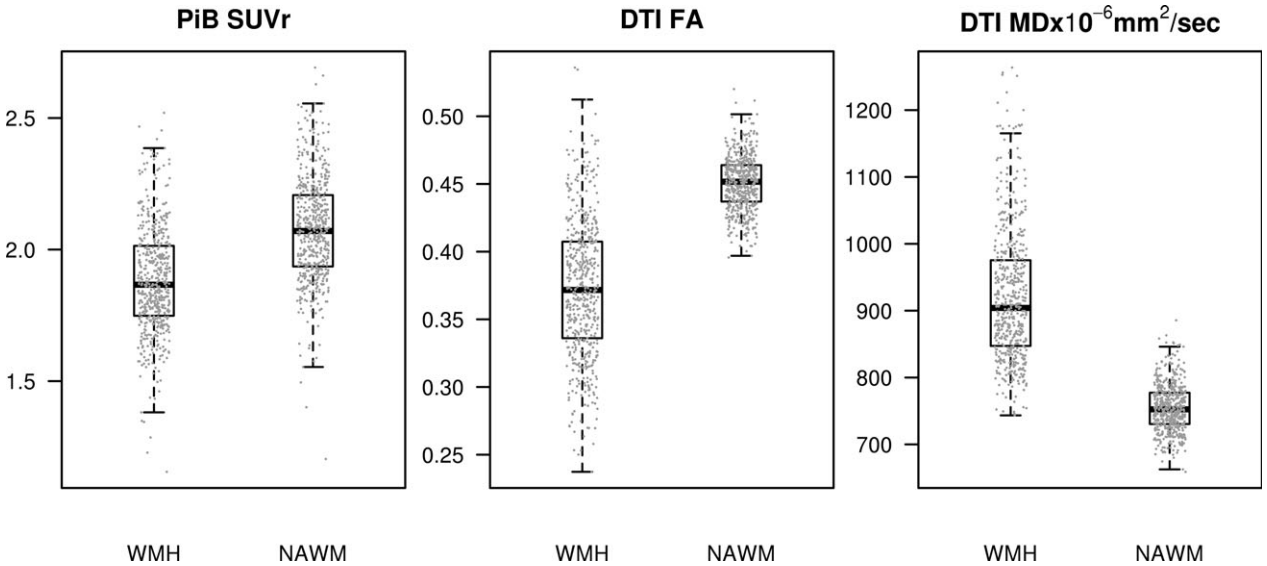

Figure 1. Box plots of Pittsburgh compound-B standard uptake value ratio and diffusion tensor imaging fractional anisotropy and mean diffusivity in white matter hyperintensities versus normal appearing white matter. DTI, diffusion tensor imaging; FA, fractional anisotropy; MD, mean diffusivity; NAWM, normal appearing white matter; PiB, Pittsburgh compound-B; SUVr, standard uptake value ratio; WMH, white matter hyperintensity.

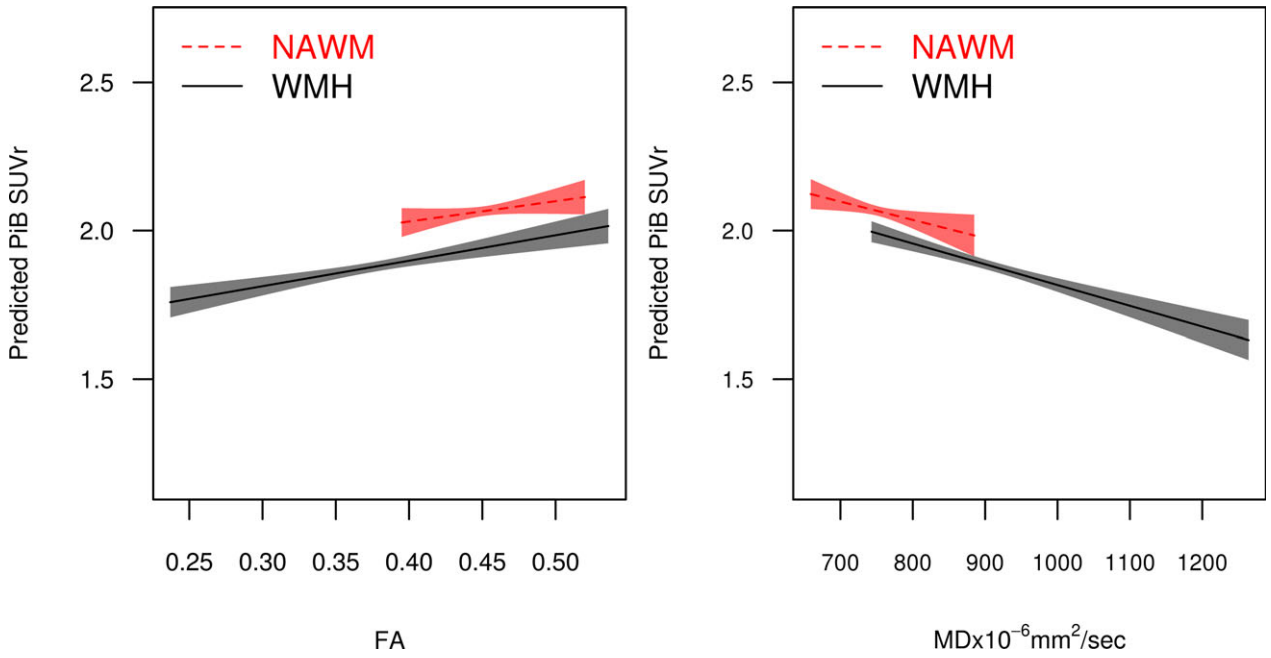

Figure 2. Associations of Pittsburgh compound-B standard uptake value ratio adjusted for age and diffusion tensor imaging fractional anisotropy and mean diffusivity in white matter hyperintensities and normal appearing white matter. Regression lines and confidence limit bands show the relationship between DTI FA and predicted PiB SUVr with age adjustment representing a 75-year-old participant. The lowest FA value detected in the NAWM was 0.40. The highest MD value detected in the NAWM was 886 mm^2/sec. FA, fractional anisotropy; MD, mean diffusivity; NAWM, normal appearing white matter; PiB, Pittsburgh compound-B; SUVr, standard uptake value ratio; WMH, white matter hyperintensity.

participants; a 67-year-old woman and an 88-year-old man, are displayed.

Associations with cognitive function

In the WMH, lower PiB SUVr was associated with lower memory ($r = 0.15$; $P < 0.001$), lower language ($r = 0.19$; $P < 0.001$), and lower global ($r = 0.14$; $P = 0.002$) cognitive function *z*-scores, after adjusting for age and global cortical PiB SUVr. Similarly, in the NAWM, lower PiB SUVr correlated with lower memory ($r = 0.11$; $P = 0.010$), lower language ($r = 0.16$; $P < 0.001$), and lower global ($r = 0.10$; $P = 0.022$) cognitive function *z*-scores after adjusting for age and global cortical PiB SUVr (Fig. 4). PiB SUVr was not associated with attention-executive function and visual-spatial function *z*-scores neither in the WMH, nor in the NAWM after adjusting for age and global cortical PiB SUVr.

In an exploratory analysis of individuals with low global cortical PiB SUVr levels (<1.42)[31] ($n = 272$), lower PiB SUVr correlated with lower global cognitive function both in the WMH ($r = 0.11$, $P = 0.08$) and NAWM ($r = 0.08$, $P = 0.20$), after adjusting for age and global cortical PiB SUVr. Although the strengths of the correlations were similar to the entire cohort, the results did not reach statistical significance.

Discussion

WM uptake is commonly observed in β-amyloid PET studies using different β-amyloid tracers, independent of cortical β-amyloid deposition, both in cognitively impaired and unimpaired individuals.[32–36] WM PiB uptake is being accepted as a reference region to normalize cortical PiB uptake on serial imaging.[1–5] However, the basis of WM PiB uptake is not yet well-understood. As a reference region for serial PET image analysis, WM seems to be more robust to imprecision in registration, less noisy due to a larger region to average the signal,[37] and have higher sensitivity due to not being at the edge of the scanner field,[4,5] in comparison to cerebellum. Thus, understanding the basis of WM PiB uptake is critical for the appropriate use of WM PiB uptake in calculations of serial PiB SUVr.

In this study, we made several critical observations: (1) While PiB SUVr in the WMH was expectedly lower compared to PiB SUVr in the NAWM, both WMH and NAWM PiB SUVrs increased with age in cognitively unimpaired older adults. (2) In the WMH, lower PiB SUVr correlated with lower FA and higher MD after adjusting for age, whereas in the NAWM, the lower PiB SUVr only correlated with higher MD, but the correlation between PiB SUVr and FA did not reach statistical

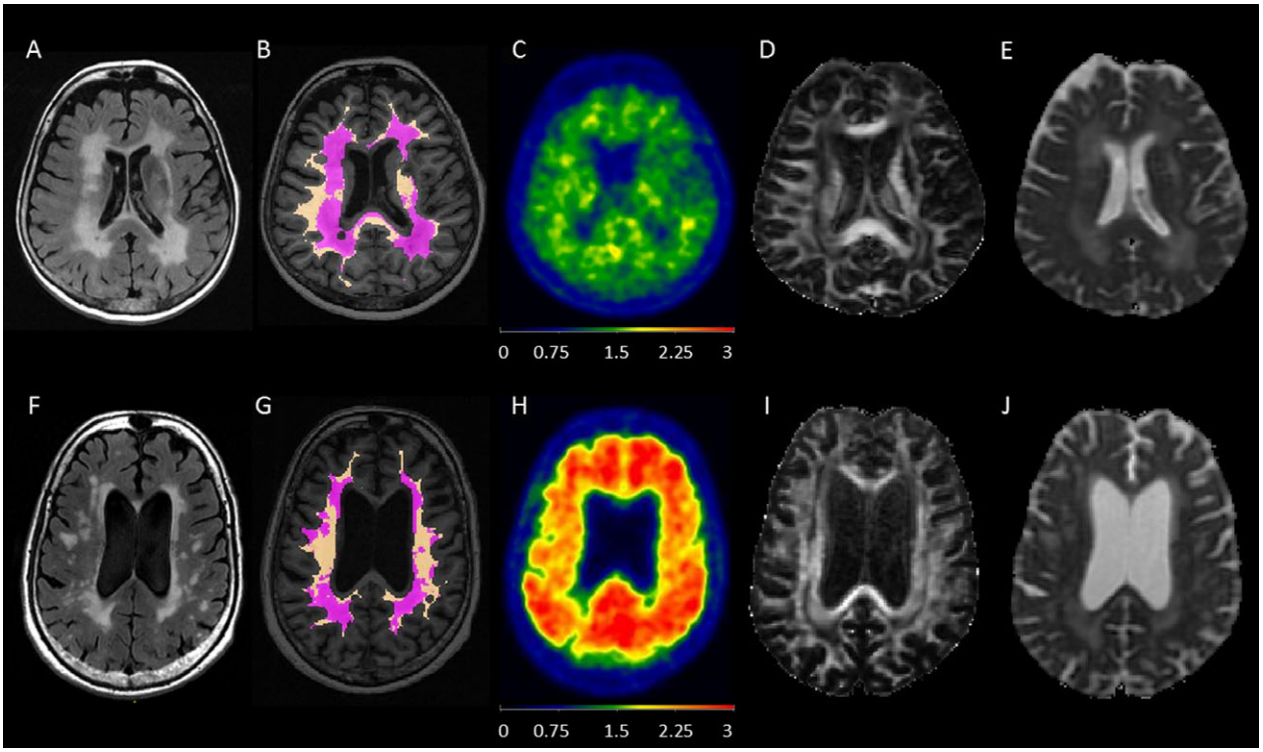

Figure 3. Examples of two participants from the cohort. Note that the WM masks were eroded by three voxels intentionally to avoid regions that are most prone to partial volume averaging with CSF and gray matter. Both participants had high WMH load observed on FLAIR-MRI, but the younger participant had higher WMH volume. They both had lower WMH PiB SUVr compared to NAWM PiB SUVr on PET, lower WMH FA compared to NAWM FA and higher WMH MD compared to NAWM MD on DTI. The older participant with high global cortical PiB SUVr had higher WMH PiB SUVr and NAWM PiB SUVr compared to the younger participant with low global cortical PiB SUVr on PET. The first participant (A–E) was a 67-year-old woman. WMH volume was 121.9 cc on T2-FLAIR-MRI (A). WMH (purple) and NAWM (copper) masks were registered and displayed on the MPRAGE image (B). On PiB PET (C); global cortical PiB SUVr was 1.21, WMH PiB SUVr was 1.38, and NAWM PiB SUVr was 1.60. On DTI (D), WMH FA was 0.27, NAWM FA was 0.40, (E) WMH MD was 1128×10^{-6} mm^2/sec and NAWM MD was 803×10^{-6} mm^2/sec. The second participant (F-J) was an 88-year-old man. WMH volume was 85.9 cc on T2-FLAIR MRI (F). WMH (purple) and NAWM (copper) masks were registered and displayed on the MPRAGE image (G). On PiB PET (H), global cortical PiB SUVr was 2.27, WMH PiB SUVr was 1.84, and NAWM PiB SUVr was 2.16. On DTI (I), WMH FA was 0.32, NAWM FA was 0.46, (J) WMH MD was 1130×10^{-6} mm^2/sec and NAWM MD was 839×10^{-6} mm^2/sec. DTI, diffusion tensor imaging; FA, fractional anisotropy; FLAIR, fluid-attenuated inversion recovery; MD, mean diffusivity; MPRAGE, magnetization-prepared rapid gradient-echo; NAWM, normal appearing white matter; PiB, Pittsburgh compound-B; SUVr, standard uptake value ratio; WMH, white matter hyperintensity.

significance. (3) Both in the WMH and in the NAWM, lower PiB SUVr, correlated with lower memory, language, and global cognitive function *z*-scores after adjusting for age and global cortical PiB SUVr.

WM PiB uptake increases with aging,[6] which is consistent with our current finding of an increase in PiB uptake both in the WMH and NAWM with age. While the basis of increasing PiB uptake in the WM with aging is not known, PiB uptake is associated with higher lipid composition of the WM, which may cause a predilection to lipophilic tracers,[38] slower blood perfusion rate[39] and therefore slower delivery of the radioligand[40] and clearance rates[41,42] compared to gray matter. Because global perfusion rate declines with aging, it is possible that age-associated decrease in global perfusion[43] and slower kinetics in the WM[39,41,42] lead to an increase in WM PiB uptake with aging. Besides perfusion and composition changes, it is also unclear if the potential change in compactness of WM with age may impact PiB uptake.

Any one of these normal aging processes may also be modified by an underlying disease process. For example, WM degeneration due to demyelinating or dysmyelinating diseases may show similar reductions of PiB uptake. In the current study, we focused on a cognitively unimpaired older cohort in order to investigate early WM alterations that relate to cognitive performance even in the absence of cognitive impairment. Our findings in the current cohort are consistent with our findings in MS with lower PiB uptake in the WMH compared to

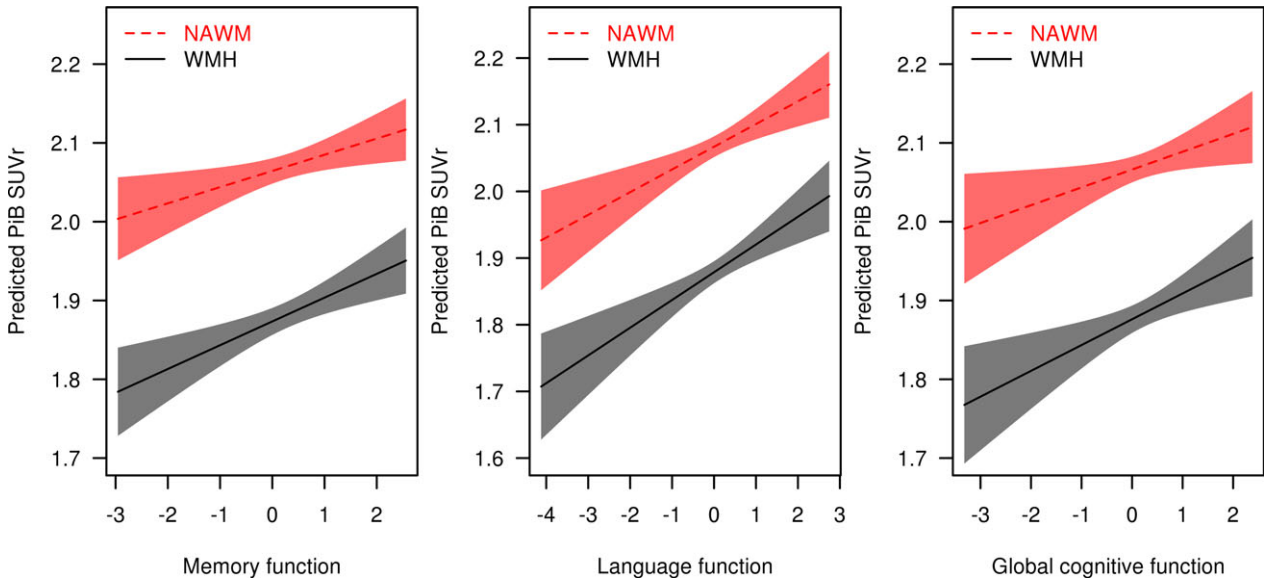

Figure 4. Associations of Pittsburgh compound-B standard uptake value ratio with memory, language, and global cognitive function *z*-scores adjusted for age and global cortical Pittsburgh compound-B standard uptake value ratio in white matter hyperintensities and normal appearing white matter. Regression lines and confidence limit bands show the relationships between memory, language, and global cognitive function *z*-scores and PiB SUVr with age and global cortical PiB SUVr adjustment representing a 75-year-old participant with a global cortical PiB SUVr of 1.50. NAWM, normal appearing white matter; PiB, Pittsburgh compound-B; SUVr, standard uptake value ratio; WMH, white matter hyperintensity.

NAWM.[12] Our findings are also consistent with recent reports on reduced PiB uptake in the WMH of older adults,[13,14] in demyelinating WM lesions of patients with MS,[7,10,11] and in animal models of demyelination.[9] It was hypothesized that PiB binds to the beta-pleated sheet of the myelin basic protein in the WM.[7] However, both the age-related myelin loss,[25,26] and the age-related increase in WMH, which in-part is associated with loss of myelin,[44,45] would cause a reduction in PiB uptake in the WM with aging. Thus, the increase in PiB uptake with aging appears to be through an independent mechanism contributing to WM PiB uptake, and competing with the decreasing PiB uptake with increasing WMH. In keeping with that, we observed an increase in PiB uptake both in the WMH and NAWM with aging. Interestingly, the increase in WMH with aging was attenuated compared to the NAWM with a statistically significant difference between the slopes, suggesting that the PiB uptake in the WMH is further modified by mechanisms that are independent of aging-related increase of PiB uptake in the WM. Overall, our data indicate that both aging and loss of WM integrity affect WM PiB uptake through competing mechanisms.

To better understand the basis of lower PiB uptake in the WMH, we studied the relationship of PiB uptake with FA and MD measurements on DTI. FA and MD measurements on DTI are widely used as biomarkers of WM integrity particularly in neurodegenerative diseases.[15,16] Furthermore, WM FA decreases and WM MD increases with increasing volume of WMH.[46,47] Previous DTI studies showed that FA in the WM tracts slowly decline after the compact myelination in the WM terminates in the fourth decade.[25,26] Furthermore vacuolation, myelin pallor and decrease in myelin density contribute to WMH on MRI in older adults.[44,45] In our study, as expected, we found lower FA and higher MD in the WMH compared to NAWM. Moreover, FA decreased and MD increased with age both in the WMH and NAWM, consistent with DTI studies in aging cohorts.[15,16] Overall, although DTI is accepted as a biomarker of WM integrity, it lacks specificity. A decline in FA may be related to both the integrity of myelin and axonal density.[48,49]

In the current study, lower PiB SUVr correlated with lower FA in the WMH, but the correlation between PiB SUVr and FA was not statistically significant in the NAWM. In contrast, lower PiB SUVr correlated with higher MD both in the WMH and NAWM. When the entire WM is analyzed as in this study, FA may have limited power in detecting WM integrity compared to MD, because FA is more prone to the influences of crossing-fibers.[50] β-amyloid PET tracers such as PiB that bind to WM as an off-target phenomenon[38,41] have been proposed as potential biomarkers of myelin integrity.[7–12,51–54]

We previously showed that PiB uptake both in the WMH and NAWM correlated with cognitive function in patients with MS.[12] In the current cohort of cognitively unimpaired older adults, lower PiB SUVr correlated with lower memory, language, and global cognitive function both in the WMH and NAWM, after adjusting for age and global cortical PiB SUVr to account for age and β-amyloid pathology that may influence global cognitive function.[27,28] Alterations in biomarkers of WM integrity on DTI precede cognitive impairment in older adults.[55] Our findings suggest that WM PiB uptake may be an early biomarker of WM integrity. Longitudinal follow-up of the current cohort is ongoing for further investigation into this possibility.

Our study did not examine whether PiB SUVr is affected differently according to the size or spatial location of WMH. It is possible that PiB SUVr may be greater in smaller WMH lesions due to their spatial smoothness or in subcortical versus periventricular versus deep WM due to partial volume averaging with NAWM. Future work will be needed to assess these questions. Even though we eroded the WM mask to avoid partial volume averaging of CSF and gray matter, with the current resolution of the PiB PET scans, partial volume averaging of CSF and gray matter PiB uptake is still possible. We observed that greater PiB uptake in the WM is associated with greater cortical β-amyloid deposition. It was recommended that WM regions close to gray matter should be avoided when WM is used as the reference region.[1,4] Thus, the rate of annual increase in WM PiB SUVr was slower when eroded subcortical WM region of interest was analyzed.[6] Furthermore, the correlation between lower PiB SUVr in the WM and lower cognitive function is opposite of the correlation that may be expected between β-amyloid deposition and cognitive function (i.e., higher cortical PiB SUVr associated with lower cognitive function). Thus, association of reduced WM PiB uptake with loss of WM integrity and lower cognitive function appears to be independent from the partial volume averaging of the cortical PiB SUVr.

Although WMH in aging is in-part associated with a decrease in myelin integrity,[44,45] the increase of PiB uptake both in the WMH and NAWM with aging suggests that additional aging-related mechanisms are influencing WM PiB uptake. Furthermore, in individuals with more WMH, the increase in WM PiB uptake with aging may attenuate. These factors should be considered when WM PiB uptake is used as a reference region for the evaluation of cortical PiB uptake. Previous studies have suggested that the rates of WM PiB SUVr increase may be minimal in the short term, such that it may be reasonable to use WM as a reference region for short-term longitudinal studies.[6] However, this may not be the case for long-term studies with increasing age and severity of WMH. Future work is needed to determine the relative rates of PiB SUVr change longitudinally in NAWM and WMH to evaluate this possibility. On the contrary, when using WM as a reference region in cross-sectional analysis, individual variability in WMH volume as well as age should be considered as variables that influence PiB SUVr.

Acknowledgments

This study was funded by the National Institutes of Health (NIH) [R01 AG040042, P50 AG016574, U01 AG006786, RF1 AG57547, C06 RR018898, R01 AG034676, R01 AG011378, R01 AG041851, R01 NS097495], the Elsie and Marvin Dekelboum Family Foundation, the Robert H. and Clarice Smith and Abigail Van Buren Alzheimer's Disease Research Program, the GHR Foundation, Mayo Foundation for Medical Education and Research, the Schuler Foundation and the Alexander Family Alzheimer's Disease Research Professorship of the Mayo Clinic. The funding sources had no role in study design, collection, analysis, interpretation, or decision to submit this paper.

Author Contributions

K.K., O.K., and B.Z. did conception and design of the study. B.Z., C.S., V.L., R.R., S.P., T.L., W.K., M.S., J.G., H.M., P.V., D.K., R.P., C.J., O.K., and K.K. did data acquisition and analyses. B.Z. and K.K. helped in drafting the manuscript, tables, and figures. C.S., V.L., R.R., M.S., J.G., H.M., P.V., D.K., R.P., C.J., and O.K. did critical revision of the manuscript.

Conflict of Interest

B Zeydan has nothing to disclose. CG Schwarz receives funding from the NIH. VJ Lowe consults for Bayer Schering Pharma, Piramal Life Sciences and Merck Research and receives research support from GE Healthcare, Siemens Molecular Imaging, AVID Radiopharmaceuticals and the NIH (NIA, NCI). RI Reid, SA Przybelski, TG Lesnick and WK Kremers have nothing to disclose. ML Senjem discloses equity/options ownership in medical companies: Gilead Sciences Inc., Inovio Pharmaceuticals, Medtronic, and PAREXEL International Corporation. JL Gunter has nothing to disclose. H Min has nothing to disclose. P Vemuri receives funding from the NIH (NIA and NINDS). DS Knopman serves on a Data Safety Monitoring Board for the DIAN study; is an investigator in clinical trials sponsored by Biogen, Lilly Pharmaceuticals and the University of Southern California; and receives research support from the NIH. RC Petersen receives funding from

the NIH, has served on the National Advisory Council on Aging and on the scientific advisory boards of Pfizer, GE Healthcare, Elan Pharmaceuticals, and Janssen Alzheimer Immunotherapy, has received publishing royalties from Oxford University Press, and has been a consultant for Roche Incorporated, Merck, Genentech, Biogen, and Eli Lily. CR Jack consults for Lily and serves on an independent data monitoring board for Roche but he receives no personal compensation from any commercial entity. He receives research support from NIH and the Alexander Family Alzheimer's Disease Research Professorship of the Mayo Clinic. OH Kantarci receives grant support from Biogen Inc. K Kantarci serves on data safety monitoring board for Takeda Global Research and Development Center, Inc, receives research support from Avid Radiopharmaceuticals and Eli Lilly, and receives funding from the NIH and Alzheimer's Drug Discovery Foundation.

References

1. Schwarz CG, Senjem ML, Gunter JL, et al. Optimizing PiB-PET SUVR change-over-time measurement by a large-scale analysis of longitudinal reliability, plausibility, separability, and correlation with MMSE. NeuroImage 2017;144(Pt A):113–127.
2. Shokouhi S, McKay JW, Baker SL, et al. Reference tissue normalization in longitudinal (18)F-florbetapir positron emission tomography of late mild cognitive impairment. Alzheimers Res Ther 2016;15:2.
3. Brendel M, Hogenauer M, Delker A, et al. Improved longitudinal [(18)F]-AV45 amyloid PET by white matter reference and VOI-based partial volume effect correction. NeuroImage 2015;108:450–459.
4. Landau SM, Fero A, Baker SL, et al. Measurement of longitudinal beta-amyloid change with 18F-florbetapir PET and standardized uptake value ratios. J Nucl Med 2015;56:567–574.
5. Chen K, Roontiva A, Thiyyagura P, et al. Improved power for characterizing longitudinal amyloid-beta PET changes and evaluating amyloid-modifying treatments with a cerebral white matter reference region. J Nucl Med 2015;56:560–566.
6. Lowe VJ, Lundt ES, Senjem ML, et al. White matter reference region in PET studies of (11)C-Pittsburgh Compound B uptake: effects of age and amyloid-beta deposition. J Nucl Med 2018;59:1583–1589.
7. Stankoff B, Freeman L, Aigrot MS, et al. Imaging central nervous system myelin by positron emission tomography in multiple sclerosis using [methyl-(1)(1)C]-2-(4'-methylaminophenyl)- 6-hydroxybenzothiazole. Ann Neurol 2011;69:673–680.
8. Wang Y, Wu C, Caprariello AV, et al. In vivo quantification of myelin changes in the vertebrate nervous system. J Neurosci 2009;29:14663–14669.
9. Faria Dde P, Copray S, Sijbesma JW, et al. PET imaging of focal demyelination and remyelination in a rat model of multiple sclerosis: comparison of [11C]MeDAS, [11C]CIC and [11C]PIB. Eur J Nucl Med Mol Imaging 2014;41:995–1003.
10. Matias-Guiu JA, Cabrera-Martin MN, Matias-Guiu J, et al. Amyloid PET imaging in multiple sclerosis: an (18)F-florbetaben study. BMC Neurol 2015;15:243.
11. Bodini B, Veronese M, Garcia-Lorenzo D, et al. Dynamic imaging of individual remyelination profiles in multiple sclerosis. Ann Neurol 2016;79:726–738.
12. Zeydan B, Lowe VJ, Schwarz CG, et al. Pittsburgh compound-B PET white matter imaging and cognitive function in late multiple sclerosis. Mult Scler 2017;01:1352458517707346.
13. Glodzik L, Rusinek H, Li J, et al. Reduced retention of Pittsburgh compound B in white matter lesions. Eur J Nucl Med Mol Imaging 2015;42:97–102.
14. Goodheart AE, Tamburo E, Minhas D, et al. Reduced binding of Pittsburgh Compound-B in areas of white matter hyperintensities. Neuroimage Clin 2015;9:479–483.
15. Maillard P, Fletcher E, Lockhart SN, et al. White matter hyperintensities and their penumbra lie along a continuum of injury in the aging brain. Stroke 2014;45:1721–1726.
16. Maniega SM, Valdes Hernandez MC, Clayden JD, et al. White matter hyperintensities and normal-appearing white matter integrity in the aging brain. Neurobiol Aging 2015;36:909–918.
17. Roberts RO, Geda YE, Knopman DS, et al. The Mayo Clinic Study of Aging: design and sampling, participation, baseline measures and sample characteristics. Neuroepidemiology 2008;30:58–69.
18. Jack CR Jr, Lowe VJ, Senjem ML, et al. 11C PiB and structural MRI provide complementary information in imaging of Alzheimer's disease and amnestic mild cognitive impairment. Brain 2008;131(Pt 3):665–680.
19. Raz L, Jayachandran M, Tosakulwong N, et al. Thrombogenic microvesicles and white matter hyperintensities in postmenopausal women. Neurology 2013;80:911–918.
20. Ashburner J, Friston KJ. Unified segmentation. NeuroImage 2005;26:839–851.
21. Schwarz CG, Gunter JL, Ward CP, et al. The Mayo clinic adult life span template: better quantification across the life span. Alzheimer's Dement 2017;13:P93–P94.
22. Reid RI, Nedelska Z, Schwarz CG, et al.; The ADNI collaboration. Diffusion specific segmentation: skull stripping with diffusion MRI data alone. In: E. Kaden, F. Grussu, L. Ning, C. Tax, J. Veraart, eds. Computational diffusion MRI mathematics and visualization. pp. 67–80. Cham: Springer, 2018.
23. Garyfallidis E, Brett M, Amirbekian B, et al. Dipy, a library for the analysis of diffusion MRI data. Front Neuroinform 2014;8:8.

24. Schwarz CG, Gunter JL, Lowe VJ, et al. A comparison of partial volume correction techniques for measuring change in serial amyloid PET SUVR. J Alzheimers Dis 2019;67:181–195.
25. Hasan KM, Kamali A, Abid H, et al. Quantification of the spatiotemporal microstructural organization of the human brain association, projection and commissural pathways across the lifespan using diffusion tensor tractography. Brain Struct Funct 2010;214:361–373.
26. Westlye LT, Walhovd KB, Dale AM, et al. Life-span changes of the human brain white matter: diffusion tensor imaging (DTI) and volumetry. Cereb Cortex 2010;20:2055–2068.
27. Mielke MM, Machulda MM, Hagen CE, et al. Influence of amyloid and APOE on cognitive performance in a late middle-aged cohort. Alzheimers Dement 2016;12: 281–291.
28. Jack CR Jr, Wiste HJ, Weigand SD, et al. Age, sex, and APOE epsilon4 effects on memory, brain structure, and beta-amyloid across the adult life span. JAMA Neurol 2015;72:511–519.
29. Fox J, Weisberg S. Mixed-effects models in R. An R companion to applied regression. 2 ed. Los Angeles, CA: Sage, 2014. p. Appendix 1–43.
30. Kokmen E, Naessens JM, Offord KP. A short test of mental status: description and preliminary results. Mayo Clin Proc 1987;62:281–288.
31. Jack CR Jr, Wiste HJ, Weigand SD, et al. Defining imaging biomarker cut points for brain aging and Alzheimer's disease. Alzheimers Dement 2017;13:205–216.
32. Lowe VJ, Lundt E, Knopman D, et al. Comparison of [(18)F]Flutemetamol and [(11)C]Pittsburgh Compound-B in cognitively normal young, cognitively normal elderly, and Alzheimer's disease dementia individuals. Neuroimage Clin 2017;16:295–302.
33. Villemagne VL, Mulligan RS, Pejoska S, et al. Comparison of 11C-PiB and 18F-florbetaben for Abeta imaging in ageing and Alzheimer's disease. Eur J Nucl Med Mol Imaging 2012;39:983–989.
34. Vandenberghe R, Van Laere K, Ivanoiu A, et al. 18F-flutemetamol amyloid imaging in Alzheimer disease and mild cognitive impairment: a phase 2 trial. Ann Neurol 2010;68:319–329.
35. Wong DF, Rosenberg PB, Zhou Y, et al. In vivo imaging of amyloid deposition in Alzheimer disease using the radioligand 18F-AV-45 (florbetapir [corrected] F 18). J Nucl Med 2010;51:913–920.
36. Forsberg A, Engler H, Almkvist O, et al. PET imaging of amyloid deposition in patients with mild cognitive impairment. Neurobiol Aging 2008;29:1456–1465.
37. Schwarz CG, Jones DT, Gunter JL, et al. Contributions of imprecision in PET-MRI rigid registration to imprecision in amyloid PET SUVR measurements. Hum Brain Mapp 2017;38:3323–3336.
38. Klunk WE, Engler H, Nordberg A, et al. Imaging brain amyloid in Alzheimer's disease with Pittsburgh Compound-B. Ann Neurol 2004;55:306–319.
39. van Gelderen P, de Zwart JA, Duyn JH. Pittfalls of MRI measurement of white matter perfusion based on arterial spin labeling. Magn Reson Med 2008;59:788–795.
40. Ibaraki M, Shimosegawa E, Toyoshima H, et al. Effect of regional tracer delay on CBF in healthy subjects measured with dynamic susceptibility contrast-enhanced MRI: comparison with 15O-PET. Magn Reson Med Sci 2005;4:27–34.
41. Fodero-Tavoletti MT, Rowe CC, McLean CA, et al. Characterization of PiB binding to white matter in Alzheimer disease and other dementias. J Nucl Med 2009;50:198–204.
42. Ichise M, Golan H, Ballinger JR, et al. Regional differences in technetium-99 m-ECD clearance on brain SPECT in healthy subjects. J Nucl Med 1997;38:1253–1260.
43. Fisher JP, Hartwich D, Seifert T, et al. Cerebral perfusion, oxygenation and metabolism during exercise in young and elderly individuals. J Physiol 2013;591:1859–1870.
44. Murray ME, Vemuri P, Preboske GM, et al. A quantitative postmortem MRI design sensitive to white matter hyperintensity differences and their relationship with underlying pathology. J Neuropathol Exp Neurol 2012;71:1113–1122.
45. Erten-Lyons D, Woltjer R, Kaye J, et al. Neuropathologic basis of white matter hyperintensity accumulation with advanced age. Neurology 2013;81:977–983.
46. Promjunyakul NO, Lahna DL, Kaye JA, et al. Comparison of cerebral blood flow and structural penumbras in relation to white matter hyperintensities: a multi-modal magnetic resonance imaging study. J Cereb Blood Flow Metab 2016;36:1528–1536.
47. Promjunyakul NO, Dodge HH, Lahna D, et al. Baseline NAWM structural integrity and CBF predict periventricular WMH expansion over time. Neurology 2018;90:e2119–e2126.
48. Song SK, Sun SW, Ju WK, et al. Diffusion tensor imaging detects and differentiates axon and myelin degeneration in mouse optic nerve after retinal ischemia. NeuroImage 2003;20:1714–1722.
49. Wheeler-Kingshott CA, Cercignani M. About, "axial" and "radial" diffusivities. Magn Reson Med 2009;61:1255–1260.
50. Jeurissen B, Leemans A, Tournier JD, et al. Investigating the prevalence of complex fiber configurations in white matter tissue with diffusion magnetic resonance imaging. Hum Brain Mapp 2013;34:2747–2766.
51. Stankoff B, Wang Y, Bottlaender M, et al. Imaging of CNS myelin by positron-emission tomography. Proc Natl Acad Sci USA 2006;103:9304–9309.

52. Wu C, Zhu J, Baeslack J, et al. Longitudinal positron emission tomography imaging for monitoring myelin repair in the spinal cord. Ann Neurol 2013;74:688–698.
53. Veronese M, Bodini B, Garcia-Lorenzo D, et al. Quantification of [(11)C]PIB PET for imaging myelin in the human brain: a test-retest reproducibility study in high-resolution research tomography. J Cereb Blood Flow Metab 2015;35:1771–1782.
54. Su Y, Wang Q, Flores S, et al. PiB PET as a biomarker for white matter integrity in aging and dementia human amyloid imaging. 2018. p. 333.
55. Zhuang L, Sachdev PS, Trollor JN, et al. Microstructural white matter changes in cognitively normal individuals at risk of amnestic MCI. Neurology 2012;79:748–754.

Supporting Information

Additional supporting information may be found online in the Supporting Information section at the end of the article.

Table S1. Results from mixed effects models testing for difference in slopes.

